3D Acoustic Metamaterial using Interconnected Helmholtz Resonators

Frieder Lucklum

Centre for Acoustic-Mechanical Microsystems (CAMM), DTU Electrical and Photonics Engineering, Technical University of Denmark (DTU), 2800 Kgs. Lyngby, Denmark; email: fluc@dtu.dk

Introduction

Helmholtz resonators are a classic acoustic sub-wavelength structure consisting of a cavity acting as acoustic compliance, a neck acting as acoustic mass, and, depending on dimensions, non-negligible viscous and thermal losses acting as acoustic dampers. They are used in various applications for sound absorption and sound insulation. As a building block in acoustic metamaterials, they have received extensive attention to optimize their geometric shape and parameters for fine tuning of resonance frequency and maximum absorption [1]. While a Helmholtz resonance can be tuned to affect very low frequencies, this effect is generally limited to a very narrow bandwidth. To overcome the bandwidth limitation, current state-of-the-art is to combine multiple resonators tuned to slightly different frequencies to combine and overlap the individual resonances [2, 3]. To further increase the bandwidth, resonance coupling has been introduced by placing the necks of adjacent resonators close to each other, so that the outer sound fields constructively and destructively interfere [4-6].

In this contribution, the concept of directly connecting Helmholtz resonators in 3D is explored, similar to elastic 3D mass-spring metamaterials [7]. To our knowledge, connected resonators as acoustic metamaterial only rarely appear in literature [8], and a systematic analysis is required to fully understand physical concepts and explore practical possibilities.

Background and Concept

To use Helmholtz resonators as a metamaterial or metasurface, repeated units are typically arranged in a periodic or semi-periodic fashion (Fig. 1.a). At resonance, the acoustic input impedance is at a minimum, allowing a maximum of air flow through the neck and compression in the cavity. The combined effect of the local resonators over a unit surface or cross-section leads to sub-wavelength absorption of sound energy and a periodic lattice as a barrier or wall leads to scattering of incident waves that prevents sound transmission.

The concept of coupled resonators is well understood in physics, e.g. for electrical or mechanical systems. Connecting two single degree-of-freedom (DOF) resonators results in a 2-DOF system that exhibits two resonances and one anti-resonance. For Helmholtz resonators, this can be achieved by connecting the neck of an adjacent resonator to the cavity of a prior resonator, effectively cascading a second acoustic mass and spring to the first (Fig. 1.b). The resulting acoustic 2-DOF system now exhibits two local minima and one local maximum in its input impedance: two coupled resonances below and above the resonance frequency of the single DOF resonator and an anti-resonance in between (Fig. 2). The first resonance appears when both resonators act in-phase, the anti-resonance at destructive opposite phases canceling the velocity in the necks, while the second resonance happens at a constructive out-of-phase pressure distribution.

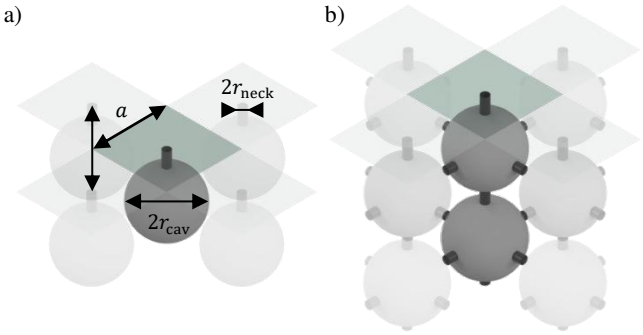

Figure 1: a) Array of single Helmholtz resonators and b) connected resonators attached to a surface (top, shaded).

In this work, all Helmholtz resonators have the same shape and dimensions unless specifically stated otherwise, with a cubic lattice constant $a = 10$ mm, cylindrical neck diameter $2r_{\mathrm{neck}} = 1$ mm, and sphere diameter $2r_{\mathrm{cav}} = 8$ mm (see Fig. 1). Table 1 lists the characteristic resonance frequencies.

Table 1: Characteristic resonance frequencies

	f_1 / kHz	f_2 / kHz	f_3 / kHz
single	1.7		
dual	1.0	2.3	2.7

The coupled in-phase resonance does not correspond to a single resonator with twice the mass and compliance, and the out-of-phase resonance is not at twice the frequency. The connection is rather a resonance cascade. Using a lumped mass-spring-damper model, Figure 3 illustrates this cascade. Here, the losses are divided into primarily viscous losses in the neck due to high tangential velocities, and primarily thermal losses in the cavity. The neck of every layer of the cascade connects to the cavity of the prior layer. This simple model does not consider in-plane connections within the same layer as illustrated in Figure 1.b. These can be added as additional cascades perpendicular to the drawing plane and again connected at the joints between neck and cavity, with the same pressure and splitting the velocity paths.

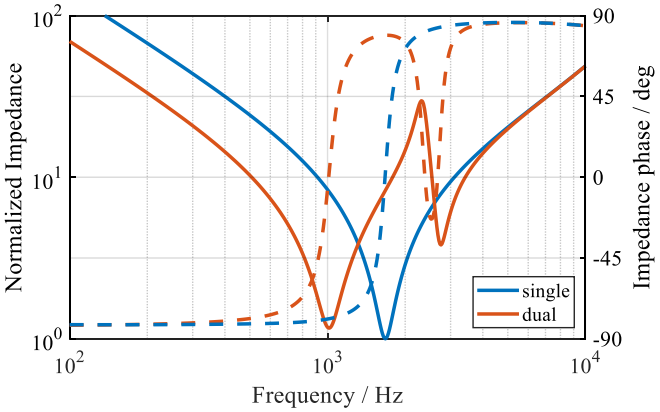

Figure 2: Normalized input impedance of single Helmholtz resonator (blue) and two connected resonators (red) that show two resonances and one anti-resonance.

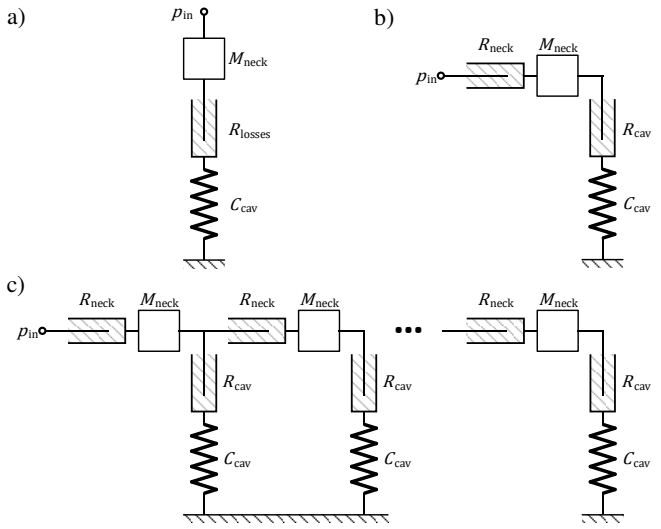

Figure 3: Equivalent lumped mass-spring-damper model for a) single resonator, b) single resonator with divided losses, and c) resonator cascade for multiple connected resonators.

In this lumped model, the acoustic mass of the neck M_{neck} and compliance of the cavity C_{cav} are calculated based on the geometric dimensions:

$$M_{\mathrm{neck}} = \frac{\rho l^*_{\mathrm{neck}}}{\pi r^2_{\mathrm{neck}}}\,, \qquad C_{\mathrm{cav}} = \frac{4\pi r^3_{\mathrm{cav}}}{3\rho c^2}\,, \tag{1}$$

with air density ρ and speed of sound c. The effective neck length l^*_{neck} considers end corrections based on the infinite baffle condition, which is a reasonably good approximation. The acoustic losses in neck R_{neck} and cavity R_{cav} are estimated to fit numerical simulations. Consequently, the acoustic input impedances of a single resonator $Z^{(1)}_{\mathrm{in}}$ and dual resonator cascade $Z^{(2)}_{\mathrm{in}}$ are:

$$Z^{(1)}_{\mathrm{in}} = Z_{\mathrm{neck}} + Z_{\mathrm{cav}} = R_{\mathrm{neck}} + \mathrm{j}\omega M_{\mathrm{neck}} + R_{\mathrm{cav}} + \frac{1}{\mathrm{j}\omega C_{\mathrm{cav}}} \tag{2}$$

$$Z^{(2)}_{\mathrm{in}} = Z_{\mathrm{neck}} + Z_{\mathrm{cav}} || Z^{(1)}_{\mathrm{in}} = Z_{\mathrm{neck}} + \frac{Z_{\mathrm{cav}} Z^{(1)}_{\mathrm{in}}}{Z_{\mathrm{cav}} + Z^{(1)}_{\mathrm{in}}}\,. \tag{3}$$

The lumped model serves as reference and validation, while the main studies utilize numerical finite element models built in COMSOL Multiphysics 6.3. Here, adjacent cavities connect to the next resonator in the surface normal direction, while periodic Floquet boundary conditions apply to lateral in-plane connections (see the non-transparent central units in Fig. 1). An infinite half-space surrounds one (for absorption studies) or both outer walls (for transmission), utilizing again Floquet periodicity at the lateral boundaries and perfectly matched layers or a plane-wave port condition normal to the outer surface. To account for viscothermal losses, the boundary layer impedance (BLI) condition applies to all solid surfaces, which is applicable since all dimensions are sufficiently large. The Helmholtz wave equation is solved in all air domains, all solid domains are rigid and not considered. The mesh consists of tetrahedral elements in the air domains with at least five elements per smallest wavelength and a mapped arrangement for PMLs. Mesh convergence studies and comparison with fully linearized Navier-Stokes solutions show very good agreement and validate the numerical model.

Sound Absorption of a Metasurface

As first application, consider a lattice of multiple layers of connected Helmholtz resonators attached to a surface that exhibits multiple sound absorption peaks. Each resonance of a cascade corresponds to a maximum in sound absorption, due to a maximum in velocity through the neck and therefore a maximum of viscous boundary losses. Figure 4 shows the absorption coefficient calculated from incident and reflected sound power in both the numerical and the lumped model for a single resonator as well as a cascade of two, three, five, and ten layers. Both results are in good agreement, the assumptions for lumped parameters, estimated losses, and periodic boundary conditions only applicable in the numerical model explain minor differences in frequencies, peak values, and bandwidth. Since this concept study uses the same resonator, individual peaks are not optimized for maximum absorption. Nevertheless, it illustrates that the frequency of the first absorption peak continuously decreases for each layer, almost up to an order of magnitude for a ten layer cascade, from 1.7 kHz down to 230 Hz. Compared to a larger Helmholtz resonator with higher acoustic mass and compliance to achieve the same low resonance frequency, the first absorption can be similar. However, higher order resonances yield wide-band absorption over multiple octave bands. Additionally, cascading does not have to extend into the depth of the solid surface. Lateral offsets or coiling arrangements are equally possible. Connecting multiple different cascades to the same surface results in a similar effect as differently tuned single resonators, combining the different individual absorption peaks into a broadband absorption envelope.

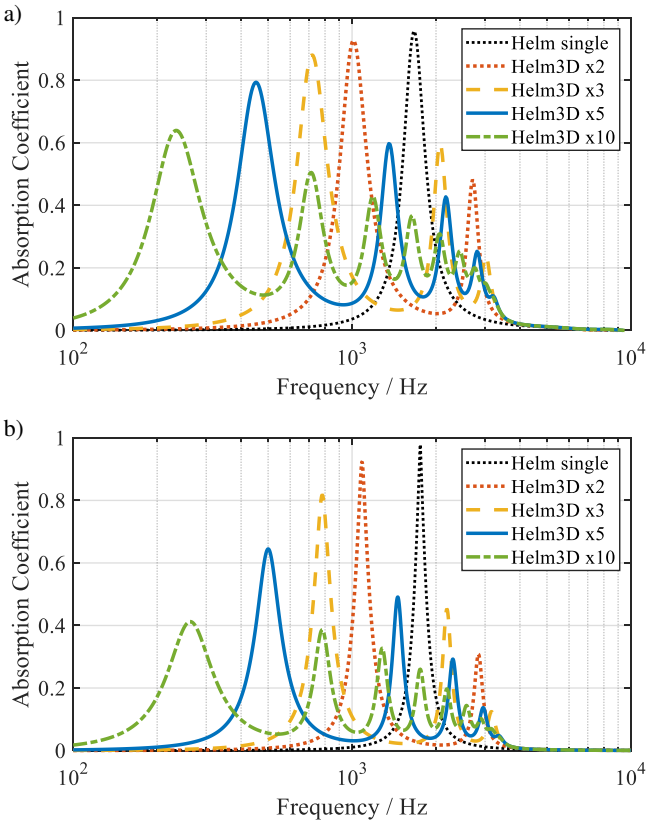

Figure 4: Absorption coefficient for a metasurface consisting of a lattice of single Helmholtz resonators and cascaded connected resonators, a) simulated with finite element model and b) calculated with lumped cascade model.

Sound Insulation of a Metamaterial

Instead of a single surface absorber, the connected Helmholtz resonators also form a lattice that can form a barrier or be integrated into a wall or panel to achieve perfect insulation. In this case, the air-filled lattice inside the panel forms an acoustic metamaterial that combines the effects of a sonic or phononic crystal with local resonances. To model this behavior, a single unit cell consisting of a spherical cavity connected with a neck in all Cartesian directions is the building block of an infinite lattice (Fig. 5.a). The resulting lattice exhibits simple cubic symmetries (Fig. 5.b). Solving the eigenvalue problem of the homogenous Helmholtz equation and using Floquet periodicity on all neck interfaces with a spatially varying wave vector k yields the acoustic band structure (dispersion diagram). This is shown in Figure 5.c, for simplicity only for the reduced Brillouin zone with the surface normal wavenumber Γ-X, the perpendicular wavenumber X-M, and the diagonal Γ-M. Dotted lines correspond to propagating modes through the lattice, where the lowest frequency mode corresponds to the fundamental Helmholtz resonances. The strong Bragg scattering of the crystal lattice results in a band gap centered around half-wavelength in respect to the lattice constant, here at 17.2 kHz, while the local resonance effects extend the gap to the sub-wavelength regime, here down to approximately 1/7th of the wavelength at 5 kHz. Further band gaps form at higher frequencies. Within these gaps, no wave propagation through the lattice is possible, it acts as a perfect reflector. Figure 6.a illustrates this effect by plotting the transmission loss calculated from incident and transmitted power for four layers of metamaterial in the surface normal direction contained in a 4 cm rigid panel. For reference, a perforated plate of the same thickness containing holes with the same size and spacing as the resonator necks is also evaluated.

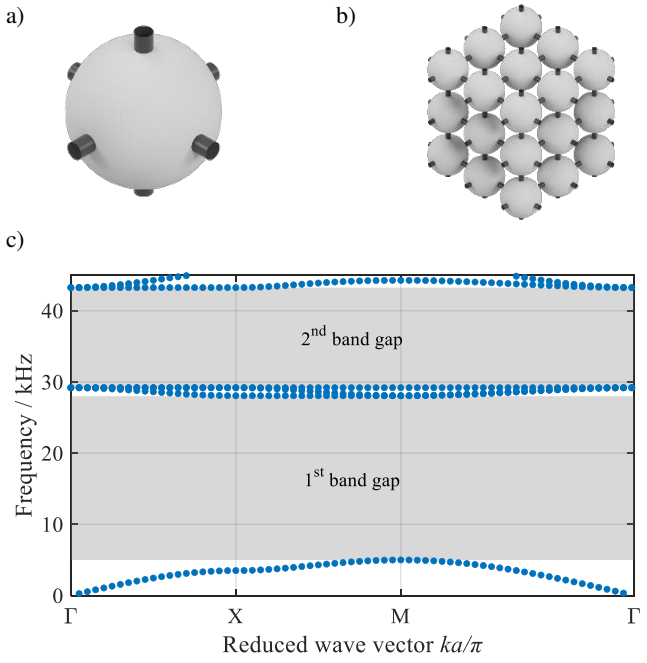

Figure 5: a) Unit cell of interconnected Helmholtz resonator metamaterial with necks in x, y, and z direction; b) Resulting lattice with simple cubic symmetries; c) Corresponding dispersion diagram (acoustic band structure) for different wave vectors highlighting the first full band gap from 5 – 28 kHz (3.5 – 28 kHz for surface normal wavenumber Γ-X).

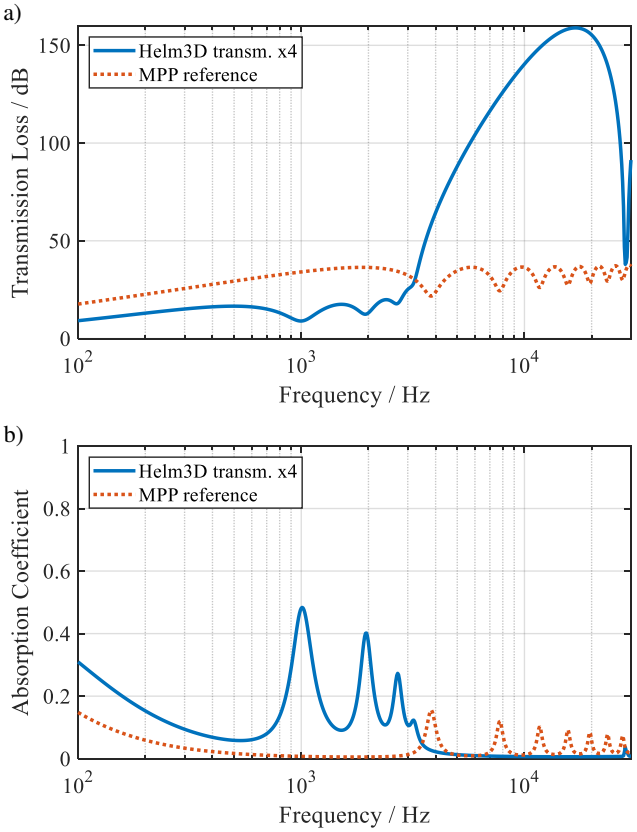

Figure 6: a) Transmission loss and b) absorption coefficient simulated for a four layer interconnected Helmholtz metamaterial through a 4 cm thick panel and a perforated plate with same hole size as the neck as reference.

At the onset of the first band gap, the normal incidence transmission loss of the metamaterial quickly surpasses the perforated plate, covering a frequency range of 3.5 – 28 kHz. In addition, the sound absorption peaks discussed in the previous section are visible as dips in the transmission loss starting at 1 kHz. Calculating the absorption coefficient from incident power minus reflected and transmitted power reveals the corresponding peaks (Fig. 6.b).

To validate the numerical studies further, selected samples were 3D-printed and measured in a cylindrical plane wave tube. Current results include transmission measurements using a 4-microphone setup according to the ASTM-E2611 standard. Due to limitations of 3D-printing and size of plane wave tubes for higher frequencies, the design was adapted to a lattice constant of $a = 6$ mm in order to fit into a tube with 15 mm diameter (upper frequency limit of 10 kHz). Besides the scaling, the cylindrical arrangement does not exhibit cubic symmetries and the solid material cannot be considered rigid. Therefore, finite element models were adapted to match the measurement conditions. A corresponding perforated plate sample was also printed, measured, and simulated as reference. Figure 7 depicts the measured and simulated transmission loss for the empty tube and for the two samples. The onset of the first band gap appears between 7 – 8 kHz here, where the connected Helmholtz resonators surpass the reference. Dips in transmission correspond to absorption peaks at the Helmholtz resonances around 4 kHz. The spurious low frequency peaks, also seen for the empty tube, are related to limitations of calibration and tube termination conditions.

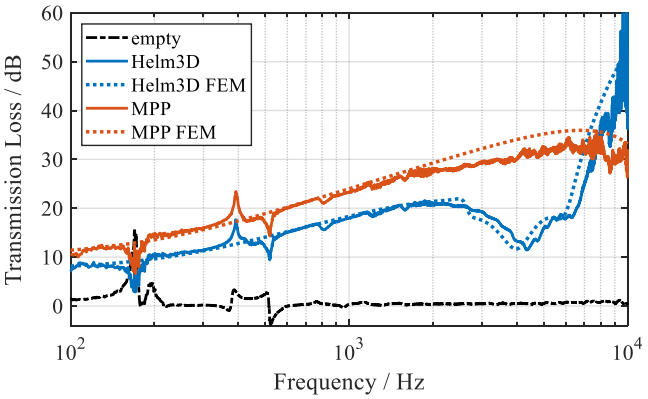

Figure 7: Measured (solid lines) and simulated (dashed) transmission loss through a cylindrical sample with 6 mm lattice size to fit into 15 mm diameter plane wave tube, with corresponding perforated plate and empty tube as reference.

The corresponding simulations show very good agreement with the measurement results and therefore validate the previous studies and the concept of interconnected Helmholtz resonators. Further measurements of absorption coefficient, acoustic impedance, as well as transmission and reflection behavior are ongoing.

Conclusions

This concept study demonstrated coupling of acoustic Helmholtz resonators by directly connecting their necks to adjacent air cavities. This forms a multi-DOF system with multiple coupled resonances and anti-resonances. By cascading multiple resonators, the frequency of absorption peaks can be lowered considerably, while also offering further peaks in a wide band. Connecting the resonators in a 3D lattice within a panel or wall yields wide band gaps for ideal sound insulation over a large frequency range. The transmission loss within the band gap is far superior to comparable perforated plates.

Further studies will focus on the opportunities provided by such a connected lattice, where each resonator and each connection can be configured and optimized to achieve targeted sound absorption and sound insulation.

References

[1] Lagarrigue, C., Groby, J.P., Tournat, V., Dazel, O., Umnova, O.: Absorption of sound by porous layers with embedded periodic arrays of resonant inclusions. J. Acoustical Society of America 134 (2013) 4670–4680. doi: 10.1121/1.4824843

[2] Jiménez, N., Romero-García, V., Pagneux, V., Groby, J.-P.: Rainbow-trapping absorbers: Broadband, perfect and asymmetric sound absorption by subwavelength panels for transmission problems. Scientific Reports 7 (2017) 13595. doi: 10.1038/s41598-017-13706-4

[3] Garza-Agudelo, D.M., Cutanda Henriquez, V., Jeong, C.-H., Andersen, P.R., Ibarias, M., Sanchez-Dehesa, J., Lucklum, F.: Metasurfaces for sound absorption over a broad range of wave incidence angle. Applied Acoustics 220 (2024) 109965. doi: 10.1016/j.apacoust.2024.109965

[4] Krasikova, M. *et al.*: Broadband noise-insulating periodic structures made of coupled Helmholtz resonators. APL Materials 12 (2024) 011115. doi: 10.1063/5.0175167

[5] Krasikova, M., Kronowetter, F., Krasikov, S., Kuzmin, M., Marburg, S., Bogdanov, A.: High-Q resonant states in coupled Helmholtz resonators. Fortschritte der Akustik – DAGA 2024.

[6] Sabat, R., Cochin, E., Kalderon, M., Lévêque, G., Antoniadis, I., Djafari-Rouhani, B., Pennec, Y.: Low frequency sound isolation by a metasurface of Helmholtz ping-pong ball resonators. J. Applied Physics 134 (2023). doi: 10.1063/5.0160267

[7] Lucklum, F., Vellekoop, M.J.: Bandgap engineering of three-dimensional phononic crystals in a simple cubic lattice. Applied Physics Letters 113 (2018) 201902. doi: 10.1063/1.5049663

[8] Liu C.R., Wu J.H., Chen X., Ma F.: A thin low-frequency broadband metasurface with multi-order sound absorption, J. Physics D: Applied Physics 52 (2019). doi: 10.1088/1361-6463/aafaa3